

Two-Plasmon Decay and Three-Halves Harmonic Generation in Filaments in a Laser-Produced Plasma

R. W. Short, W. Seka, K. Tanaka, and E. A. Williams^(a)

Laboratory for Laser Energetics, University of Rochester, Rochester, New York 14627

(Received 4 November 1983)

The two-plasmon decay of light propagating in filaments in a laser-produced plasma and the resulting $3\omega_0/2$ light emission is discussed with use of a simplified model. Experimental observations are consistent with the predictions of the model. Implications for use of the $3\omega_0/2$ doublet splitting as a temperature diagnostic are discussed.

PACS numbers: 52.35.Mw, 52.40.Db, 52.50.Jm

The two-plasmon decay (TPD) instability in laser-produced plasmas is of interest both as a potential source of hot electrons¹ and as a source of half-harmonic light ($\omega_0/2$, $3\omega_0/2$, etc.) which may be useful as a coronal temperature diagnostic.^{2,3} The simplest signature of TPD is the generation of $3\omega_0/2$ light,³ which is produced by the "addition" of a decay plasmon to a laser photon; $\omega_0/2$ light is more difficult to analyze since it is not only generated by "subtraction" of a decay plasmon from a laser photon, but also by linear conversion of TPD plasmons to photons and directly by absolute Raman scattering.

Previous theoretical investigations³⁻⁶ of the generation of $3\omega_0/2$ light by TPD have assumed that the decay occurs near the quarter-critical surface of the bulk plasma density profile, which is modeled as a planar expansion with density gradient parallel to the incident wave vector \vec{k}_0 . The most satisfactory of these theories seems to be that of Gusakov,⁵ in which plasmons from TPD with maximum growth rate propagate through the density profile to a point at which their wave vectors satisfy the \vec{k} -matching conditions for combination with a laser photon, generating a $3\omega_0/2$ photon. The predicted spectrum of $3\omega_0/2$ emission is a doublet split symmetrically by $\pm\Delta$ from the exact $3\omega_0/2$ frequency, where

$$\begin{aligned} \Delta/\omega_0 &= (3v_T^2 k_0^2 / 2\omega_0^2) (1 + 12 \sin^2 \theta)^{1/2} \\ &\approx 2.2 \times 10^{-3} (1 + 12 \sin^2 \theta)^{1/2} T(\text{keV}). \end{aligned} \quad (1)$$

Here v_T is the thermal electron velocity, \vec{k}_0 is the laser light wave vector at quarter-critical density, and θ is the observation angle measured from target normal, which we assume is antiparallel to the density gradient. This result agrees well with our experimental results at $1.05 \mu\text{m}$ on spherical targets, though the angular dependence could not be determined. In our $0.35\text{-}\mu\text{m}$ experiments on planar tar-

gets, however, the two peaks are strongly asymmetric, with the red shift several times larger than the blue shift; very little angular dependence of the splitting is observed. The above mentioned theories predict symmetric shifts (except for Barr's,⁶ which predicts a larger blue shift), and strong angular dependence.

These discrepancies have led to the consideration of an alternative model, wherein TPD occurs in high-intensity, low-density light filaments. The filaments are formed by the self-focusing of "hot spots" in the incident laser beam (which have much higher relative intensity in our $0.35\text{-}\mu\text{m}$ experiments than at $1.05 \mu\text{m}$). If the background plasma density outside the filament is greater than quarter-critical, a cylindrical quarter-critical surface is formed inside the filament at which TPD can occur. Direct evidence that TPD does occur in filaments is provided by the experiments of Baldis and Corkum,⁷ in which the resulting decay plasmons were observed by Thomson scattering of a probe laser. The observations indicated a quarter-critical surface extending from the critical to quarter-critical regions of the background plasma, and clearly associated with the presence of hot spots in the incident beam. Further evidence is provided by the angular distribution of $\omega_0/2$ light in oblique-incidence experiments,⁸ by observations of filamentary structures in spatially resolved $3\omega_0/2$ images,⁹ and by numerical simulations.¹⁰

To estimate thresholds and growth rates for TPD in a filament and to determine the characteristics of the resulting $3\omega_0/2$ emission we employ a simplified model: We neglect the curvature of the filament wall (which should be valid for filament radii larger than a wavelength) and we neglect the radial variation of the laser light intensity (which should be small over the narrow region near quarter-critical where TPD is localized). The model thus consists of a plasma slab (representing the wall of the fila-

ment) with a linear density gradient, $n_0(x) = n_0(1 + x/L)$. The uniform-amplitude pump wave has its wave vector, \vec{k}_0 , perpendicular to the density gradient. Since the region in which the instability occurs has only a small radial extent in the filament, we look for modes which are absolute (i.e., nonpropagating) in the direction of the density gradient.

These modes may be found by the method originated in Ref. 4, where the plasma wave equations are Fourier transformed in space and time and the existence of absolute modes is shown to correspond to the existence of bound-state eigenfunctions in \vec{k} space of a Schrödinger equation with a potential $F(\vec{k}, \omega)$, \vec{k} and ω being the wave vector and frequency of one of the decay plasmons. The term of F of highest order in the large parameter k_0L may be written¹¹

$$F_0(\vec{k}, \Omega) = \alpha^2 \left[\frac{k_0^2 \kappa^2 (\vec{k} \cdot \hat{v}_0)^2}{k^2 (\vec{k} - \vec{k}_0)^2} + \beta (\Omega - \kappa)^2 \right], \quad (2)$$

where $\alpha = (4k_0v_0/\omega_0)k_0L$, $\beta = 9v_T^4k_0^2/v_0^2\omega_0^2$, $\Omega = \omega_0(\omega - \omega_0/2)/(3v_T^2k_0^2)$, $\kappa = \vec{k} \cdot \vec{k}_0/k_0^2 - \frac{1}{2}$, and \vec{v}_0 is the quiver velocity of electrons in the pump field.

The fastest growing modes which are absolute in the \hat{x} direction are found by taking \vec{k} in the \vec{v}_0 - \vec{k}_0 plane and solving

$$F_0(\vec{k}, \Omega)|_{\vec{k}_a, \Omega_a} = \partial F_0 / \partial k_x |_{\vec{k}_a, \Omega_a} = 0, \quad (3)$$

for k_{ax} and Ω_a as functions of κ . The inhomogeneous correction to the mode frequencies to next lower order in k_0L is given by¹¹

$$\Omega_1 = (n + \frac{1}{2})k_0 \left[\frac{(-2 \partial^2 F_0 / \partial k_x^2)^{1/2}}{\partial F_0 / \partial \Omega} \right]_{\vec{k}_a, \Omega_a}.$$

Here n is a nonnegative integer which denotes discrete eigenfunctions in the potential F . Since the effect of inhomogeneity is to decrease the length of plasma over which the wave-vector-matching conditions can be satisfied,¹² Ω_1 can only decrease the growth rate, and hence we take $n=0$ to obtain the most unstable mode. As in the case of normal incidence¹¹ the next-lower-order term in the potential, F_1 , may be shown to vanish when (3) is satisfied; in fact this is true for the TPD potential for arbitrary angles of incidence.¹³

After some algebra, we obtain the frequencies of

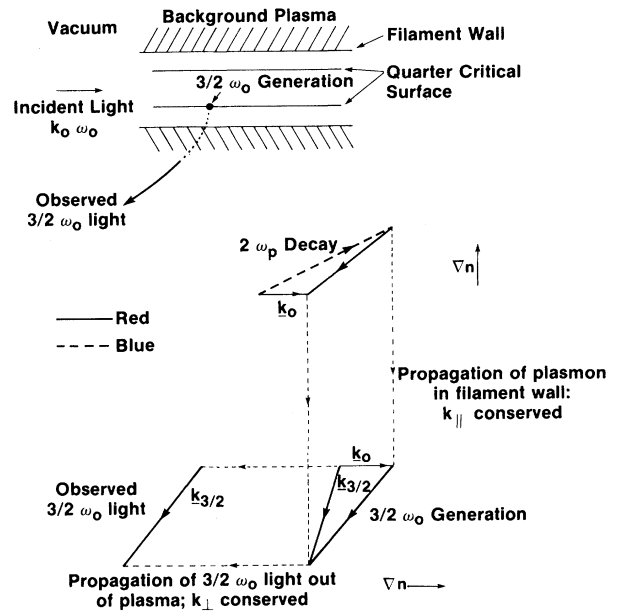


FIG. 1. Wave-vector diagram for $3\omega_0/2$ generation. The upper triangle represents the two-plasmon decay. The lower-frequency ("red") plasmon is shown propagating in the radial density profile to a point where its \vec{k} adds to \vec{k}_0 to produce a $\vec{k}_{3/2}$ which satisfies the dispersion relation for $3\omega_0/2$ light. This light then propagates out of the filament and out of the plasma to the observation point.

the most unstable absolute mode:

$$\frac{\omega}{\omega_0} = \frac{1}{2} \pm 3 \frac{v_T 2k_0^2}{\omega_0^2} \kappa + i \frac{2}{3} \frac{k_0 v_0}{\omega_0} \left(1 - \frac{1}{\alpha \kappa} \right), \quad (4)$$

where a positive imaginary part indicates instability. The last term represents the inhomogeneous correction.

Instability requires $\alpha \kappa > 1$, which is always satisfied for decays with large enough κ 's. Landau damping limits the size of k and therefore κ , however; requiring $k_0 \kappa \lambda_D \leq 0.2$ yields the threshold condition $(v_0/v_T)k_0L \geq 2.5$. In a filament we expect the light pressure inside to balance the plasma pressure outside, so that $v_0/v_T \sim 1$, and the radial scale length should be larger than a wavelength, so that $k_0L \geq 2\pi$. Thus the threshold condition for TPD inside filaments is readily satisfied.

Figure 1 illustrates the generation of the redshifted $3\omega_0/2$ light. The lower-frequency plasmon from TPD propagates in the filament wall to a density where its wave vector can add to \vec{k}_0 to generate a $3\omega_0/2$ photon. To produce backscattered light, as shown here, \vec{k} must be large enough to cancel the inward-directed \vec{k}_0 . Plasmons with smaller \vec{k} 's gen-

erate forward-scattered red light. The component of the $3\omega_0/2$ wave vector perpendicular to $\vec{k}_0 = k_0\hat{x}$ is $k_\perp = (3\omega_0/2c)\sin\theta$. This component is invariant as the $(3\omega_0/2c)$ light propagates in the bulk plasma density profile $n_0(x)$. Thus at the background density n_0 where the $3\omega_0/2$ light is generated, the component of the wave vector parallel to \vec{k}_0 is given by $k_\parallel^2 = (3\omega_0/2c)^2(1 - 4n_0/9n_c) - k_\perp^2 = (\frac{9}{4}\cos^2\theta - n_0/n_c)\omega_0^2/c^2$. If we neglect the small refraction in the boundary of the filament (where the density gradient changes from being parallel to \vec{k}_0 on the outside to perpendicular to \vec{k}_0 on the inside), k_\parallel will be the same inside the filament, so that the parameter κ for the red component of the $3\omega_0/2$ doublet is

$$\kappa_{\text{red}} = \left| \frac{3}{2} \pm \left(\frac{9}{4}\cos^2\theta - \frac{n_0}{n_c} \right)^{1/2} \frac{\omega_0}{k_0c} \right|, \quad (5)$$

where the $+$ ($-$) sign corresponds to backward (forward) scattering, and the resulting frequency shift is given by $\Delta = (3v_T^2 k_\perp^2 / \omega_0) \kappa$. Near $\theta \sim \pi/2$ the planar expansion model for the bulk plasma becomes invalid. If the target is overdense, the forward-scattered light is reflected at its critical surface and observed in combination with the back-scattered light. However, if the target is underdense, the forward-scattered light can be observed separately in the forward direction. The value of k_0 depends on the detailed radial structure of the filament; from Anderson,¹⁴ however, we have to good approximation

$$\omega_0/k_0c \approx (1 - 0.8n_0/n_c)^{-1/2}, \quad (6)$$

for filaments with $v_0/v_T \sim 1$. Using (6) and noting¹¹ that $\kappa \geq 0.5$ for the absolute mode, we see from (5) that $\theta \leq 137^\circ$ for forward scatter (180° representing the direction of \vec{k}_0). Thus the red peak should be excluded from a cone angle of about 43° around the forward direction. This is confirmed by the data shown in Fig. 2(b); for an underdense target the red component of $3\omega_0/2$ is seen at 135° but is greatly reduced at 173° . The small amount of red light observed at 173° can be ascribed to convective TPD modes with $\kappa < 0.5$ and smaller growth rates.

From (4) we see that larger κ 's give larger growth rates for TPD. The maximum κ for forward scatter at 135° is $\kappa \approx 0.71$ at $n_0/n_c = 1$; however, this value is quite sensitive to angle. If we average over $\pm 5^\circ$, to allow for small deviations from planar geometry, we get $\kappa \approx 1$, corresponding to a wavelength shift $\Delta\lambda_{3/2}/\lambda_L = 5.2 \times 10^{-4} T(\text{keV})$, where λ_L is the vacuum laser wavelength. For backscatter κ is larger and has only a weak dependence on background

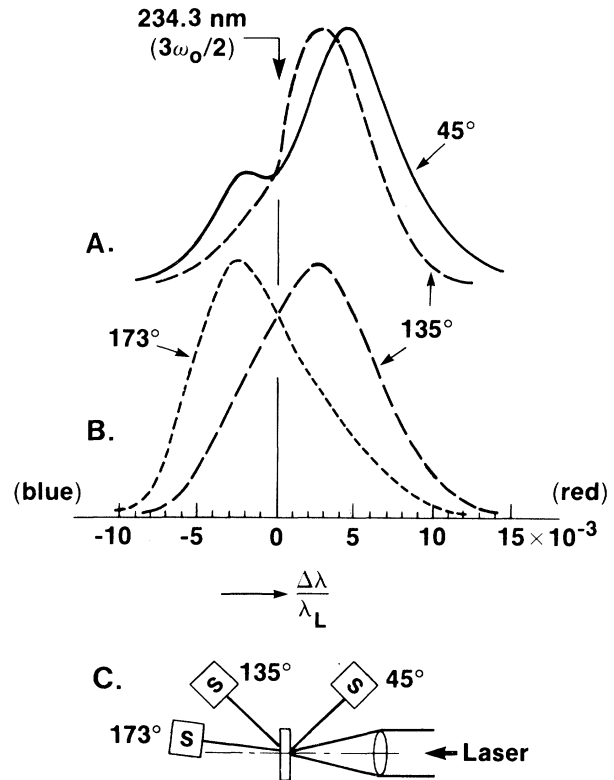


FIG. 2. Observation of $3\omega_0/2$ spectra in planar uv laser plasmas. (a) Spectra from an overdense target observed at 45° (solid line) and an underdense target observed at 135° (dashed line). (b) Spectra from an underdense target observed at 173° (dotted line) and 135° (dashed line). (c) Experimental setup.

density, so that we expect the red $3\omega_0/2$ component to be generated along the whole length of the filament from critical to quarter-critical. Taking the midpoint of this range, $n_0/n_c = \frac{5}{8}$, and $\theta = 45^\circ$ as a representative point, we find from (5) that $\kappa = 2.5$; κ varies by less than 10% from this value over the length of the filament. The angular dependence is also weak, and this is in accord with our experimental observations of backscatter, which see little or no angular dependence of the splitting. Using $\kappa \approx 2.5$ to estimate the backscatter red shift, we get $\Delta\lambda_{3/2}/\lambda_L \approx 3.3 \times 10^{-3} T(\text{keV})$.

Comparison with the experimental results in Fig. 2(a) yields temperatures of 1.8 keV for the average coronal temperature (from the 45° peak) and 4.8 keV in the critical region (from the 135° peak). The latter result may overestimate the maximum temperature in the filament since it assumes that the filament passes through a region where $n_0/n_c \approx 1$. The result is fairly sensitive to the maximum density assumed; if we take $(n_0/n_c)_{\text{max}}$

$= 0.9$, the temperature corresponding to the observed shift would be 3.4 keV. However, since the light intensity in the filament increases at higher background densities, while thermal conduction decreases, it is reasonable to expect higher local temperatures to be associated with filaments in higher background densities. The coronal temperature obtained from hydrocode simulations for these experimental parameters is about 2 keV, in good agreement with the average coronal temperature obtained from the red component of backscatter.

A similar analysis can be applied to the blue component. Using (6) and the condition $k_0 + k_{\parallel} < k_{3/2}$, we obtain the requirement

$$\left(\kappa + \frac{3}{2}\right)^2 \leq \frac{\frac{9}{4} - n_0/n_c}{1 - 0.8n_0/n_c}.$$

Since $\kappa \geq 0.5$ this leads to the condition $n_0/n_c \geq 0.8$ for blue-component generation. Also, since both the laser photon and the blue-shifted plasmon wave vectors are directed forward, the blue light is generated only at shallow angles ($\leq 26^\circ$) to the filament axis. Under these circumstances it is likely that most of the blue component is trapped in the filament and propagates as though in a waveguide. In an overdense target we expect the blue $3\omega_0/2$ light to spray out from the termination of the filament near the critical surface, and then as a result of refraction and reflection from the $\frac{3}{4}$ -critical surface to be observed in a wide range of backscatter angles; this accounts for the blue peak at 45° in Fig. 2(a). For an underdense target, the blue light should propagate through the target within the filament and be observed only in a narrow range around the forward direction. This expectation is confirmed by the spectra in Fig. 2(b), which show only a blue peak at 173° and only a red peak at 135° . For the blue component the maximum κ is $\kappa = 1$, again at $n_0/n_c = 1$, so that the blue component should have a shift equal to that of the forward-scattered red component. This is also confirmed by the spectra in Fig. 2(b). Our observations of the blue component thus provide further evidence that filaments extend into critical density, rather than breaking up at lower densities because of various proposed instabilities.¹⁵

In conclusion, we have derived a threshold condition which indicates that TPD should occur in self-focused light filaments. The predicted angular dis-

tribution and spectral characteristics of the resulting $3\omega_0/2$ light are in good agreement with our experimental observations. As a practical consequence, the shift of the backscattered red component should be a more reliable coronal temperature diagnostic than the total splitting of the $3\omega_0/2$ doublet when filamentation is present. Conversely, an asymmetric $3\omega_0/2$ doublet may be interpreted as a signature of filamentation.

This work was partially supported by the U.S. Department of Energy Inertial Fusion Project under Contract No. DE-AC08-80DP40124.

(a)Present address: Lawrence Livermore National Laboratory Livermore, Cal. 94550.

¹H. A. Baldis and C. J. Walsh, *Phys. Fluids* **26**, 1364 (1983); D. W. Phillion, E. M. Campbell, K. G. Estabrook, G. E. Philips, and F. Ze, *Phys. Rev. Lett.* **49**, 1405 (1982); N. A. Ebrahim, H. A. Baldis, C. Joshi, and R. Benesch, *Phys. Rev. Lett.* **45**, 1179 (1980).

²A. N. Starodub and M. V. Filippov, *Fiz. Plazmy* **5**, 1090 (1979) [*Sov. J. Plasma Phys.* **5**, 610 (1979)].

³A. I. Avrov, V. Yu. Bychenkov, O. N. Krokhin, V. V. Pustovalov, A. A. Rupasov, V. P. Silin, G. V. Sklizkov, V. T. Tikhonchuk, and A. S. Shikanov, *Zh. Eksp. Teor. Fiz.* **72**, 970 (1977) [*Sov. Phys. JETP* **45**, 507 (1977)].

⁴C. L. Liu and M. N. Rosenbluth, *Phys. Fluids* **19**, 967 (1976).

⁵E. Z. Gusakov, *Pis'ma Zh. Tekh. Fiz.* **3**, 1219 (1977) [*Sov. Tech. Phys. Lett.* **3**, 504 (1977)].

⁶P. D. Carter, S. M. L. Sim, H. C. Barr, and R. G. Evans, *Phys. Rev. Lett.* **44**, 1407 (1980); H. C. Barr, Rutherford Laboratory Annual Report, 1979 (unpublished), Sec. 8.33.

⁷H. A. Baldis and P. B. Corkum, *Phys. Rev. Lett.* **45**, 1260 (1980).

⁸W. Seka *et al.*, *Bull. Am. Phys. Soc.* **27**, 909 (1982).

⁹M. J. Herbst, J. A. Stamper, R. R. Whitlock, R. H. Lehmberg, and B. H. Ripin, *Phys. Rev. Lett.* **46**, 328 (1981).

¹⁰A. B. Langdon and B. F. Lasinski, *Phys. Rev. Lett.* **34**, 934 (1975).

¹¹A. Simon, R. W. Short, E. A. Williams, and T. Dewandre, *Phys. Fluids* **26**, 3107 (1983).

¹²C. S. Liu, M. N. Rosenbluth, and R. B. White, *Phys. Fluids* **17**, 1211 (1974).

¹³B. B. Afeyan, E. A. Williams, R. W. Short, and A. Simon, *Bull. Am. Phys. Soc.* **27**, 951 (1982).

¹⁴D. Anderson, *Phys. Scr.* **18**, 35 (1978).

¹⁵C. E. Max, Lawrence Livermore Laboratory Report No. UCRL 53107, 1982 (unpublished), Vol. 1, pp. 39-40.